Society For Biomaterials

Bacteriostatic behavior of surface modulated silicon nitride in comparison to polyetheretherketone and titanium

Ryan M. Bock,[1] Erin N. Jones,[1] Darin A. Ray,[1] B. Sonny Bal,[1,2] Giuseppe Pezzotti,[3] Bryan J. McEntire[1]

[1]Amedica Corporation, 1885 W. 2100 S, Salt Lake City, Utah 84119
[2]Department of Orthopaedic Surgery, College of Medicine, University of Missouri, Columbia, Missouri 65212
[3]Ceramic Physics Laboratory, Kyoto Institute of Technology, Sakyo-ku, Kyoto, Matsugasaki 606-8585, Japan

Received 30 September 2016; revised 23 November 2016; accepted 15 December 2016
Published online 00 Month 2017 in Wiley Online Library (wileyonlinelibrary.com). DOI: 10.1002/jbm.a.35987

Abstract: Perioperative and latent infections are leading causes of revision surgery for orthopaedic devices resulting in significant increased patient care, comorbidities, and attendant costs. Identifying biomaterial surfaces that inherently resist biofilm adhesion and bacterial expression is an important emerging strategy in addressing implant-related infections. This *in vitro* study was designed to compare biofilm formation on three biomaterials commonly employed in spinal fusion surgery—silicon nitride (Si_3N_4), polyetheretherketone (PEEK), and a titanium alloy (Ti6Al4V-ELI) —using one gram-positive and one gram-negative bacterial species. Disc samples from various surface treated Si_3N_4, PEEK, and Ti6Al4V were inoculated with 10^5 CFU/mm^2 *Staphylococcus epidermidis* (ATCC®14990™) or *Escherichia coli* (ATCC®25922™) and cultured in PBS, 7% glucose, and 10% human plasma for 24 and 48 h, followed by retrieval and rinsing. Vortexed solutions were diluted, plated, and incubated at 37 °C for 24 to 48 h. Colony forming units (CFU/mm^2) were determined using applicable dilution factors and surface areas. A two-tailed, heteroscedastic Student's *t*-test (95% confidence) was used to determine statistical significance. The various Si_3N_4 samples showed the most favorable bacterial resistance for both bacilli tested. The mechanisms for the bacteriostatic behavior of Si_3N_4 are likely due to multivariate surface effects including submicron-topography, negative charging, and chemical interactions which form peroxynitrite (an oxidative agent). Si_3N_4 is a new biomaterial with the apparent potential to inhibit biofilm formation. © 2017 Wiley Periodicals, Inc. J Biomed Mater Res Part A: 00B:000–000, 2017.

Key Words: silicon nitride, anti-infective, surface treatments, titanium, polyetheretherketone

How to cite this article: Bock RM, Jones EN, Ray DA, Sonny Bal B, Pezzotti G, McEntire BJ. 2017. Bacteriostatic behavior of surface modulated silicon nitride in comparison to polyetheretherketone and titanium. J Biomed Mater Res Part A 2017:00A:000–000.

INTRODUCTION

Perioperative and latent infections are leading causes of revision surgery for orthopaedic devices, with reported rates of between 2.7 and 18%.[1,2] Their occurrence is distressing to both the recipient of the prosthesis and surgeon alike, resulting in increased patient hospitalization and comorbidities, with attendant health-care expenditures that can range up to 4.8 times the cost of the index surgery.[3] Furthermore, nosocomial infections are a growing problem due to both patient demographics and the rising antibiotic resistance of bacteria to germicidal therapies.[4–7] To maintain or improve their quality of life, an increasing number and percentage of older patients are undergoing arthroplastic procedures for the spine and other total joints, leading to a higher incidence of prosthetic joint infections (PJI).[7] Furthermore, according to a recent summarized report from the World Health Organization, over-prescription or excessive self-medication of antibiotics in humans, their overuse in animals and agriculture, and a lack of new antibacterial compounds are increasing the number and variety of highly-virulent microbial strains.[8] Governmental health-care organizations are grappling with both the technical and logistical enormity of this impending worldwide threat, as well as the financial burdens that may likely be incurred.[9] Indeed, we are entering a new era in germicidal warfare due to both the declining availability and effectiveness of antibiotic remedies. By necessity, this new era will have to rely on innovative alternative therapies.[8]

One potential therapy which has garnered considerable interest is the use of biomaterials that possess inherent bacteriostatic properties.[10,11] These materials provide physical or chemical barriers to surface adhesion by an individual bacterium. As indicated in Figure 1, attachment is the initial step in acquisition of a prosthetic joint infection.[12] Attachment may be followed by reversion to a planktonic condition, or these pathogens can remain dormant on the surface for hours, days, weeks, or even years, until the biological milieu is ripe for biofilm creation.[13] In subsequent steps,

Correspondence to: Bryan J. McEntire, e-mail: BMcEntire@amedica.com

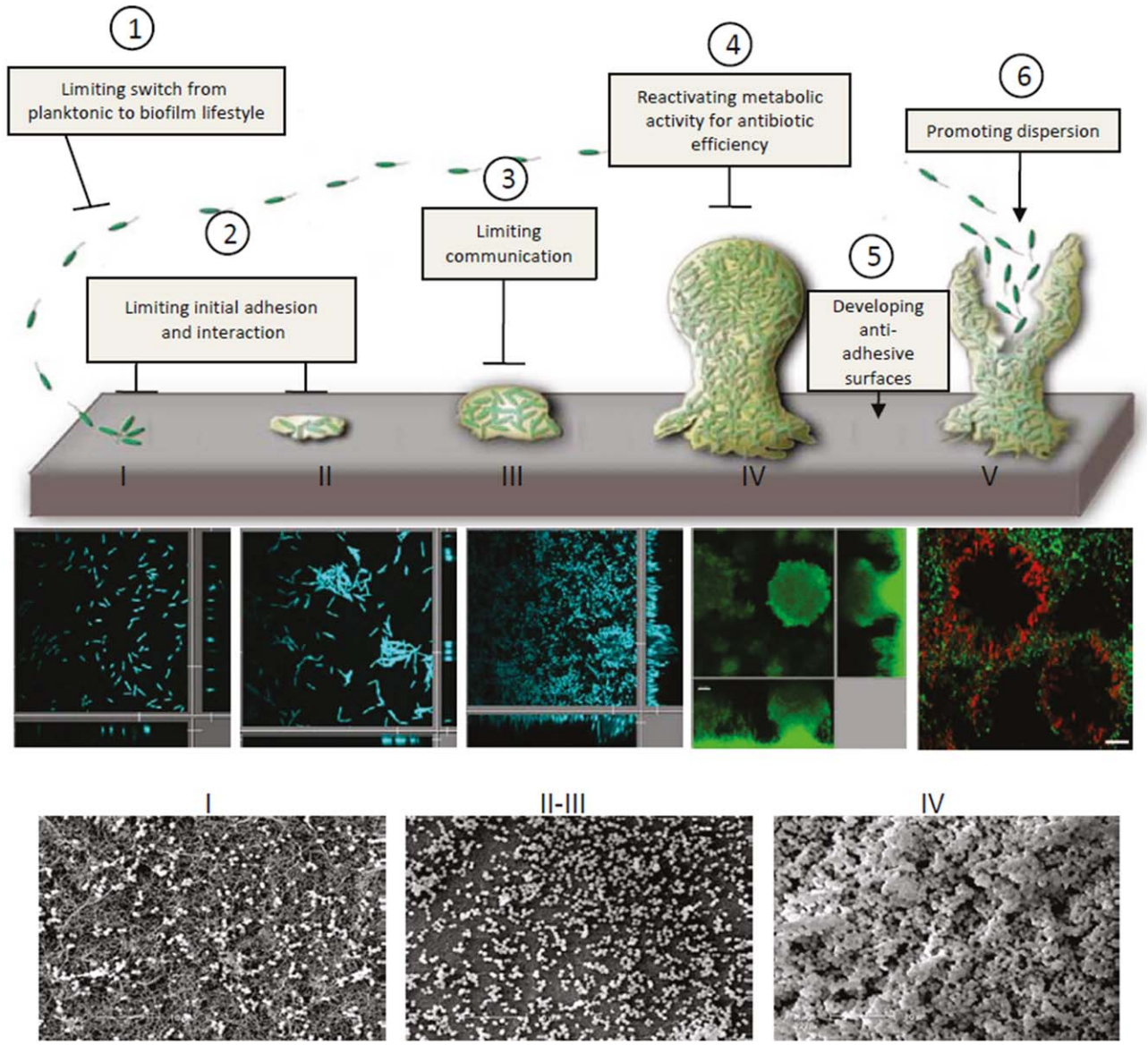

FIGURE 1. Sequential life events for a bacterial biofilm: (I) Initial attachment of planktonic bacteria to a surface; (II-III) Quorum sensing and establishment of a community; (IV) Formation of an extracellular polysaccharide membrane, internal proliferation, and maintenance; and (V) Release and dispersion of planktonic bacteria back into the environment. Steps 1–5 are areas where strategies for interrupting the processes involved with bacterial biofilm formation can be implemented. (Illustration courtesy of Ref. 12, Reprinted with permission.).

the biofilm begins to form with quorum sensing (that is, attraction and adhesion of other individual bacterium to form a community), which is followed by the establishment of a tough extracellular polysaccharide (EPS) matrix or slime in which bacterial cell proliferation occurs. The entrained bacteria comprise only about 15 volume % of the biofilm while the slime accounts for the balance.[14] The EPS is unique in that it is highly resistant to both common and advanced antimicrobial treatments.[15] In fact, entrenched biofilms require up to 1000-times the antibiotic dosage necessary to combat planktonic bacteria.[10,16] Consequently, the ensuing inflammation typically leads to a chronic infection which can only be eliminated by revision surgery involving removal of the contaminated implant, debridement of affected hard and soft tissues, prolonged administration of local and systemic antibiotics, and replacement of the prosthesis only when the pathogen has been eradicated.[17] Unfortunately, while this aggressive treatment is effective in curing the infection, it carries the risk of poorer functional results.[18] With this in mind, employing biomaterials that are resistant to initial biofilm formation are of increasing importance. Recent reviews have elucidated strategies for development of these types of antimicrobial devices.[10,11,19,20] They range from active implants that elute bactericidal compounds (for example, silver, zinc, copper, iodine, vancomycin, and so forth) and those that possess non-leachable contact surface biocides (for example, chitosan, peptides, quaternary amines, and *N*-halamines) to more passive implants that rely on the material's inherent surface chemistry or topography.[10,21] In fact, many of these passive strategies are

bioinspired; they seek to mimic the antibacterial capabilities of mineral or organic substances found in nature.[22–24] Bacteriostasis is the term often used to describe these passive approaches to biofilm prevention. It is defined as the capability of a material to metabolically interfere with bacteria to prevent its attachment, growth, or reproduction. Note that this definition differs markedly from bactericides, which are designed to kill the microorganisms upon contact. Surface chemical composition, dissolution characteristics (i.e., corrosion), hydrophilicity, and roughness or porosity are believed to play important roles in bacteriostasis.[25] Although there are many exceptions, general guidelines suggest that bacteriostatic materials are typically corrosion resistant, hydrophilic, and have a negative surface charge and/or chemical moieties which electrostatically or chemically repel adhesion by the bacterium's pili or fimbriae.[13,26] To a lesser extent, irregular surface texture is thought to promote bacterial attachment due to greater surface area (that is, aspirates and depressions) for colonization. Machining grooves or scratches of the material surface on the order of the bacteria's size are believed to encourage adhesion, although nanostructured topography has been found to have the opposite effect.[27,28]

Ceramics are considered to be more effective than metals or plastics in resisting biofilm formation. Ceramics are generally hydrophilic, less susceptible to corrosion (that is, bioinert), with many having negatively charged surfaces; and they can be polished to extremely smooth finishes, all of which purportedly provide bacteriostatic benefits.[13] While metals can also be produced to high surface finishes, they are typically less hydrophilic, are more susceptible to corrosion, and, depending upon composition, generally have positively-charged surfaces.[29] In fact, some metallic implants (for example, screws and plates) are often modified via application of a hard PVD ceramic coating (for example, TiN, TiCN, and so forth) in order to eliminate bacterial attachment or microbial influenced corrosion.[25] Synthetic nonresorbable polymers (for example, polyether ether ketone, polyethylene, polyurethane, polymethylmethacrylate, and so forth) can be moderately- to highly-hydrophobic, possess a broad range of surface roughness values, and are neutrally-charged or have functional chemical groups which provide either positive or negative surface charge; all of which have been shown to either support or hinder attachment of negatively-charged bacteria.

In this study, an *in vitro* test was developed to compare biofilm formation on three biomaterials commonly used in spinal fusion surgery – polyetheretherketone (PEEK), a titanium alloy (Ti6Al4V-ELI), and silicon nitride (Si_3N_4) – using gram-positive (*Staphylococcus epidermidis*) and gram-negative (*Escherichia coli*) bacterial species. These two microbes were selected because they are easily studied within the laboratory (that is, biosafety level 1) and are among the common causes of PJI for their respective genus.[30,31] This is a follow-up to earlier studies which also examined the anti-infective behavior of these three biomaterials.[32,33] However, the present investigation was expanded to include a broad range of surface modulated Si_3N_4 samples.[34] Being a non-oxide ceramic, Si_3N_4's surface composition can be readily altered from one that is rich in silicon-amines (Si-NH_2) which protonate to form Si-NH_3^+ at physiologic pH, to one consisting primarily of silanols (Si-OH) which deprotonate to form Si-O^-. Its surface topography can also be modified from an "as-fabricated" material which has a fibrous texture to one that is ultra-smooth, achieved through fine grinding and polishing. Prior to conducting the *in vitro* bacterial tests, these materials were characterized for their morphological, chemical, wetting, and charging properties using scanning electron microscopy (SEM), white-light interferometry, X-ray photoelectron spectroscopy (XPS), sessile drop techniques, and streaming potential measurements, respectively, in an attempt to assess how these properties might influence bacterial interaction and adhesion.

MATERIALS AND METHODS

Silicon nitride material and sample preparation

The silicon nitride used in these studies was produced by Amedica Corporation (Salt Lake City, UT, USA). Details of its processing and basic properties are provided elsewhere.[34,35] This biomaterial has a nominal composition of 90 weight % (wt %) Si_3N_4, 6 wt % yttrium oxide (yttria, Y_2O_3), and 4 wt % aluminum oxide (alumina, Al_2O_3). The Y_2O_3 and Al_2O_3 are necessary densification additives. During sintering, these two oxides combine with a minor amount of Si_3N_4 and with native silicon dioxide (silica, SiO_2) present as a protective oxide layer on the Si_3N_4 particles to form an intergranular glassy or partially crystalline oxynitride phase commonly referred to as SiYAlON. Therefore, the dense bioceramic is actually a composite consisting of about 90 volume % (vol %) polycrystalline Si_3N_4 grains and 10 vol % SiYAlON intergranular glass. Although these two constituents are intricately intermixed at the micrometer scale, each exhibits unique surface chemistry, which in turn may affect bacterial adhesion. From this base silicon nitride composition, a large quantity of identical disc samples (Ø12.7 × 1 mm) were prepared from one powder lot and separated into four groups for characterization and biological testing. These four groups were subjected to different post-densification surface treatments in order to modify their surface chemistry or morphology, as follows:[34]

As-fabricated Si_3N_4 (Af-Si_3N_4 or Af-SN). The as-fabricated group consisted of samples which had no post-densification surface treatments. This untreated group served as a comparative baseline or control for the remaining three Si_3N_4 groups.

N_2-Annealed Si_3N_4 (N_2-Si_3N_4 or N_2-SN). The N_2-SN group of samples was subjected to a post-densification heat-treatment in flowing N_2 gas (~1.1 bar) at 1400 °C for 30 min. This treatment had the effect of increasing the fraction of SiYAlON glass at the surface of the ceramic samples.

Glazed Si_3N_4 (Gl-Si_3N_4 or Gl-SN). To further characterize the impact that the SiYAlON phase might have on

bacteriostatic behavior, a compositionally identical powder frit of SiYAlON was separately prepared and dip coated onto this group of Si_3N_4 discs. The frit was subsequently fired onto the samples in flowing N_2 gas (~1.1 bar) at 1400 °C for 30 min.

Oxidized Si_3N_4 (Ox-Si_3N_4 or Ox-SN). This group of samples was subjected to firing in air at 1070 °C for 7 h. This treatment resulted in an increased concentration of silanol (Si-OH) groups on the surface of the samples.

In addition to these Si_3N_4 samples, two dimensionally identical groups of discs were prepared from PEEK (ASTM D6262, Ketron®PEEK 1000, Quadrant EPP USA, Inc., Reading PA, USA distributed by McMaster-Carr, Santa Fe Springs, CA, USA) and a titanium alloy (ASTM F136, Ti6Al4V-ELI, distributed by Vincent Metals, Minneapolis, MN, USA). Although there have been a number of recent compositional modifications or surface enhancements to both PEEK and titanium,[36–38] these two groups were chosen as being representative of the two biomaterials traditionally utilized in spinal fusion surgery. They served as additional controls along with the Af-Si_3N_4 group. Future studies may examine selected surface-modified PEEK and titanium for their bacteriostatic characteristics.

Sample characterization methods

Scanning electron microscopy (SEM). SEM evaluations were performed using a field emission gun scanning electron microscope (FEG-SEM) (Quanta, FEI, Hillsboro, OR, USA). All samples were sputter-coated (108auto, Cressington, Watford, UK) with a thin (≈20–30 Å) layer of gold. The discs were imaged using an accelerating voltage of 10 kV at working distances of 7–10 mm and spot sizes of 4–4.5 mm.

White-light interferometry (WLI). Surface morphology data were obtained using a white light interferometer (NewView 5000, Zygo, Middlefield, CT, USA). Data from a 0.285 mm by 0.214 mm field of view was captured using a 20× Mirau objective lens and a 2.0 multiplier. The MetroPro software package (ver. 8.1.5, Zygo, Middlefield, CT, USA) was used to calculate roughness parameters (that is, average, R_a, and root mean square, R_q) and generate surface roughness plots from the captured data.

Wetting angle measurements. An optical comparator (2600 Series, S-T Industries, St. James, MN, USA) with built-in goniometer functionality was used to measure static contact angles of deionized water droplets having fixed volumes (VWR Signature Variable Volume Pipette, VWR, Radnor, PA, USA) of 25 μL. Both sides of each droplet's projected image were measured, and at least eight measurements per condition were taken.

Zeta potential measurements. Streaming potential analyses were performed using an electrokinetic analyzer (SurPASS, Anton-Paar USA, Ashland, VA, USA). A background electrolyte of 1 mM KCl which exhibited a natural pH of 5.5 was used in all experiments, which were divided into two runs. The first run took measurements across a pH range of 3–5.5 using auto-titration of 0.1M HCl solution to control pH. The second run used a new solution of background electrolyte for measurements across a pH range of 5.5–10 and auto-titration of 0.1M NaOH solution to control pH. Each run contained two material samples. Observed streaming potentials were converted to zeta (ζ) potentials using the Helmholz-Smoluchowski equation.[39]

X-ray photoelectron spectroscopy (XPS). A spectrometer (Axis Ultra, Kratos, Manchester, UK) was employed with an Al-kα monochromatic X-ray source to determine the elemental surface chemistry of each group of discs. Low resolution spectrum scans were conducted using a pass energy of 160 eV, with a compositional resolution of approximately 0.1 atomic percent (at %). High resolution scans bracketing peaks of interest (which were expected to improve the compositional resolution to approximately 0.01 at %.) were conducted using a pass energy of 40 eV. The analysis area was set to the spectrometer's maximum (700 μm × 300 μm) in order to average differences between the composition within grains and the intergranular phase. Data obtained were processed using commercially-available software (CasaXPS, Casa Software Ltd., UK). Usage of a low energy electron source and application of ultra-high vacuum-rated colloidal silver (Ted Pella, Inc., Redding, CA, USA) to the contact points between the samples and the fixture were employed to mitigate charging effects. Following argon sputtering to remove adsorbed surface contaminants, all reported data were obtained at a beam energy of 4.2 keV, a gun angle with respect to each sample of 45°, a raster area of 3 mm^2, and a sample current of approximately 2 μA.

Bacterial adhesion and proliferation testing

Sample cleaning and sterilization. After preparation, treatment, and characterization of the various Si_3N_4, PEEK, and Ti6Al4V discs, all samples were sequentially ultrasonically cleaned in ethanol and deionized water for 5 min each (Branson Ultrasonics, Danbury, CT, USA). They were then UV-C sterilized (254 nm, Phillips, Denver, CO, USA) for 30 min. A one hour waiting period was observed after sterilization to allow the surfaces to equilibrate, especially on titanium, as UV exposure has been shown to increase surface free radicals within the protective oxide layer on titanium.[40]

Bacterial media preparation and inoculation. The medium employed in the bacterial experiments was designed to simulate physiologic fluids, without the presence of cells. Phosphate buffered saline (PBS) was used to mimic blood ion concentrations; 7% glucose was added as an energy source and 10% human plasma was included as a source of proteins. Inclusion of proteins was essential because they reportedly immediately coat the implant's surface and therefore can influence bacterial attachment.[41] Separate media were inoculated with one colony of either *Escherichia coli* (*E. coli*, ATCC®25922™) or *Staphylococcus epidermidis* (*S. epidermidis*, ATCC®14990™) and cultured on

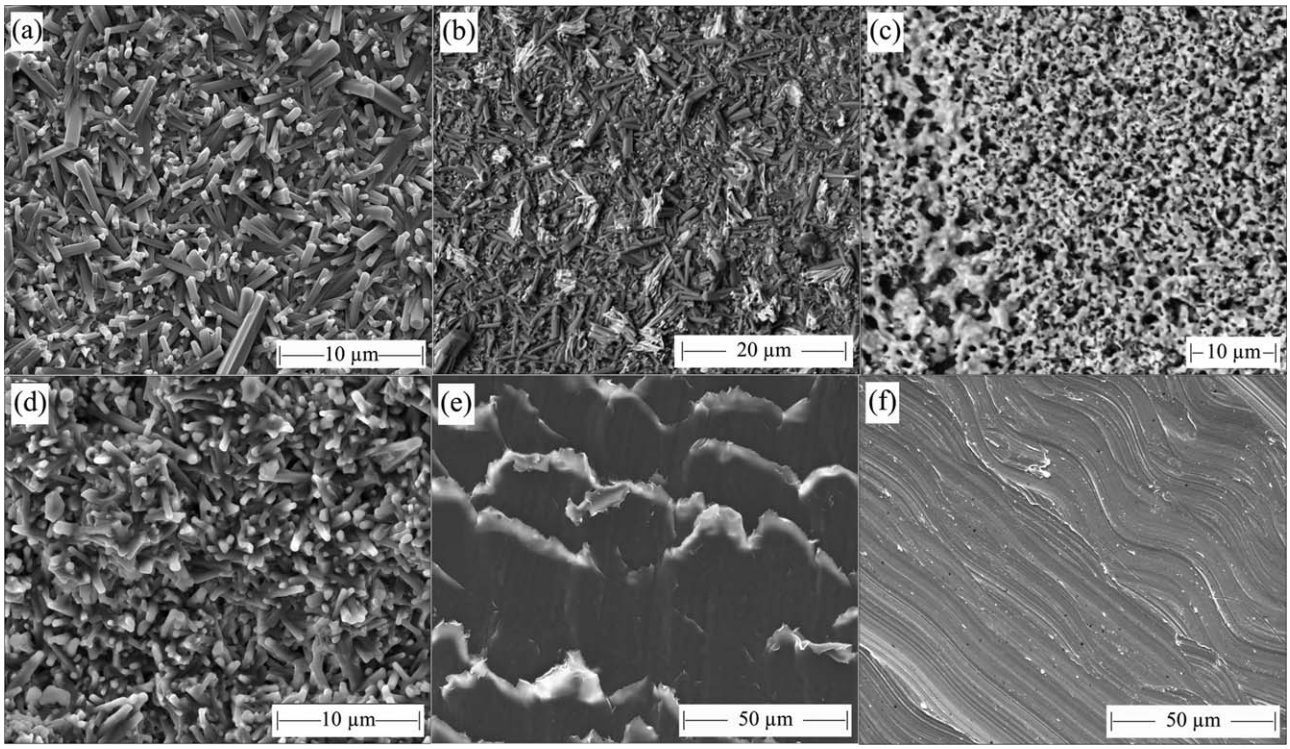

FIGURE 2. SEM photographs of: (a) Af-Si_3N_4, (b) N_2-Si_3N_4, (c) GI-Si_3N_4, (d) Ox-Si_3N_4, (e) PEEK, and (f) Ti6Al4V.

a shaking incubator (Southwest Science, Hamilton, NJ, USA) at 37 °C and 175 rpm for 24 h until a concentration of 10^5 cells/mL of growth had been achieved. Then, each disc was inoculated with the bacterial solution within individual well plates. The well plates were subsequently placed on the shaking incubator for 24 h or 48 h at 37 °C and 120 rpm. All 48 h coupons underwent a media refresh at 24 h (7 mL) to eliminate the possibility of nutrient insufficiency affecting the results.

Bacterial extraction, plating, and counting. Samples were removed at either 24 h or 48 h and rinsed with 5 mL of PBS in a fresh well plate on the shaking incubator for 2 mins at 120 rpm. Samples were subsequently gently dip-rinsed in PBS to remove planktonic bacteria and placed in a 50 mL centrifuge tube along with 10 mL of fresh PBS, which was followed by vigorous vortexing for 2 mins. The bacterial solution was serially diluted as necessary (that is, 1/10×, 1/100×, 1/1,000×, and 1/10,000×) and plated onto Petrifilm™ (6400/6406/6442 Aerobic Count Plates, 3M, Minneapolis, MN, USA). The Petrifilm™ was incubated at 37 °C (10–180 E, QuincyLab, Inc., Chicago, IL, USA) for 24 and 48 h in stacks of <20 films. At the end of each period, the number of colonies on each Petrifilm™ was counted and recorded. The results were multiplied by applicable dilution factors and divided by surface area to determine the average colony forming units per square millimeter (CFU/mm^2). A two-tailed, heteroscedastic Student's *t* test (95% confidence) was used to determine statistical significance.

RESULTS

Surface topography

Provided in Figure 2 are SEM images of the various treated Si_3N_4 samples along with PEEK and Ti6Al4V. The as-fabricated Si_3N_4 of Figure 2(a) exhibited a typical acicular grain structure consisting of protruding anisotropic hexagonal ß-Si_3N_4 grains within an oxide intergranular matrix, having prismatic dimensions of ~0.2 to 2.0 μm in cross-section by ≤ 10 μm in length. Note that many of these grains extend well above the nominal material surface. The N_2-annealed Si_3N_4 [Figure 2(b)] had a similar acicular structure; but it was interspersed with islands of SiYAlON (that is, the lighter contrasting phase). These islands have higher concentrations of the Al_2O_3 and Y_2O_3 sintering aids intermixed within an oxynitride glass. Figure 2(c) shows the morphology of the SiYAlON coating onto the as-fabricated base Si_3N_4. In this instance, the SiYAlON is highly porous, and appears to be a combination of both vitreous and crystalline phases. The oxidized Si_3N_4 surface shown in Figure 2(d) has similar morphology to the as-fabricated base material. However, closer inspection reveals the presence of an amorphous second phase (assumed to be the oxide layer) covering each individual grain and spanning between grains. Finally, shown in Figure 2(e,f) are photographs of machined PEEK and Ti6Al4V, respectively. In contrast to the Si_3N_4 samples, which had roughness at the micron- and submicron-scales, the topographies of the PEEK and Ti-alloy specimens were much larger and characteristic of typically machined surfaces. In both instances, their macro-surface roughness was generated by an identical tool path during machining. The surface roughness values of the various samples, as

TABLE I. Summary of the white light interferometry average (R_a) and root-mean-square (R_q) surface roughness for the Si_3N_4, PEEK, and Ti6Al4V samples

Material	R_a (nm)	R_q (nm)
PEEK	819	1,034
Gl-Si_3N_4	785	1,094
Af-Si_3N_4	641	830
Ox-Si_3N_4	568	745
N_2-Si_3N_4	509	654
Ti6Al4V	377	494
Polished-Si_3N_4	2	5

measured by white light interferometry, are provided in Table I. The data are arranged in descending order of average roughness. For reference purposes, a polished-Si_3N_4 sample was also characterized and included in Table I, demonstrating that an ultra-smooth surface can be achieved for this dense bioceramic.

Shown in Figure 3(a∼f) are oblique topographical plots for each material from the white-light interferometer. These quantitative results confirm the qualitative observations provided in Figure 2(a∼f). At the micron- and submicron-levels, the Si_3N_4 samples generally had the highest surface roughness values whereas the Ti-alloy was the smoothest. The PEEK material is an obvious exception. Its high apparent roughness is due to fewer features (of larger size), which were likely due to brittle fracture and shear occurring during the machining process [∼10 to 20 μm, compare Figure 2(e) and Figure 3(a)] when compared with either the Si_3N_4 or Ti-alloy samples. In contrast, the Ti-alloy had a uniform repetitive pattern to its surface, consistent with a strain-hardening chip removal process.

Zeta-potential

Provided in Figure 4 are the results of streaming potential measurements converted to zeta-potentials (ζ) for the various Si_3N_4 samples as a function of pH. Isoelectric points (IEP) determined from these curves provided values of 4.6, 4.5, and 3.1 for the N_2-SN, Af-SN, and Ox-SN samples, respectively. ζ-potential curves for PEEK and the Ti-alloy are also shown in the graph, but these data were adapted from previous publications utilizing the same streaming potential measurement technique and background electrolyte.[42,43] Their IE*P* values were 3.9 and 4.4, respectively. Perhaps more interesting are the ζ-potentials exhibited by these various materials at homeostatic pH (that is, ∼7.4). These results indicate that the Ox-SN sample had the largest

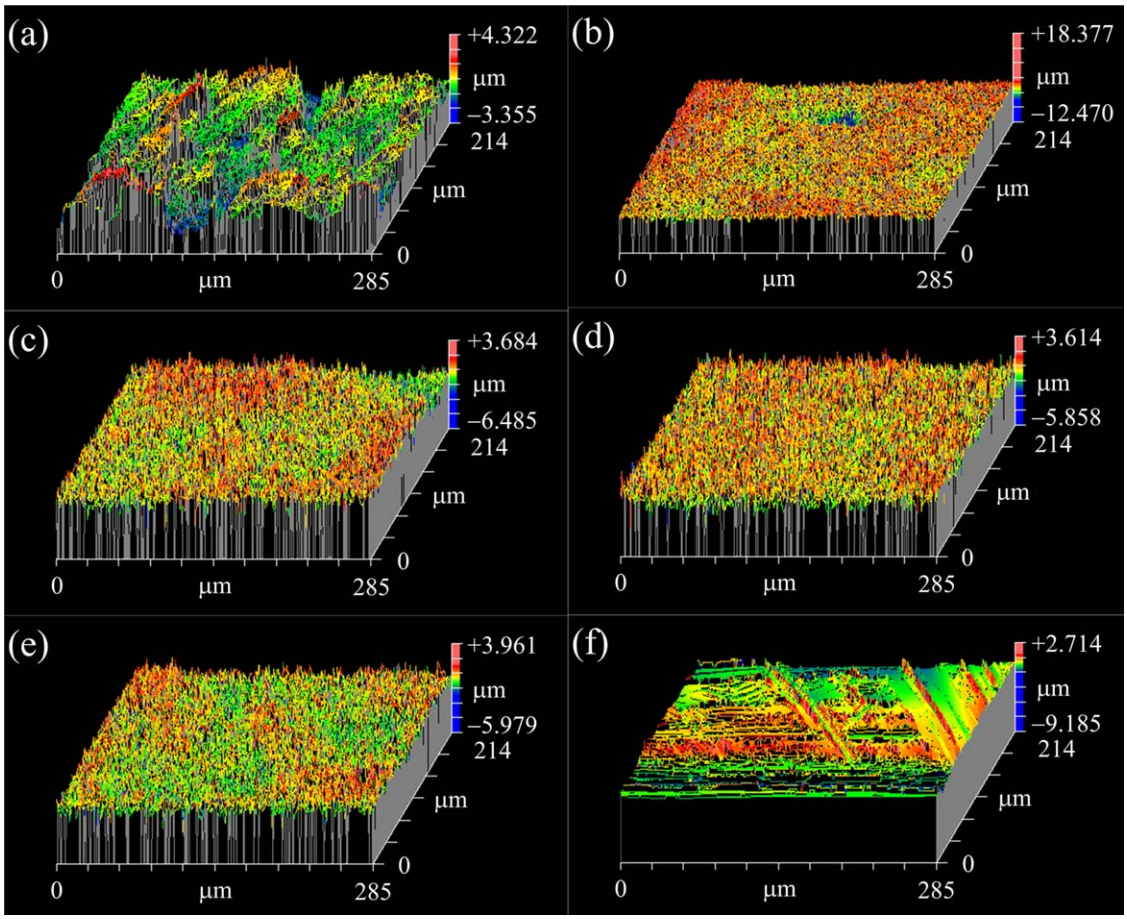

FIGURE 3. White light interferometer oblique topographical plots of: (a) PEEK, (b) Gl-Si_3N_4, (c) Af-Si_3N_4, (d) Ox-Si_3N_4, (e) N_2-Si_3N_4, and (f) Ti6Al4V.

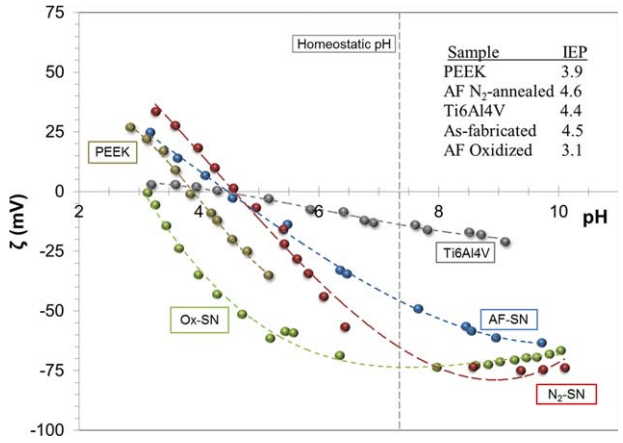

FIGURE 4. Zeta potential as a function of pH, as measured by streaming potential for Af-Si_3N_4, N_2-Si_3N_4, Ox-Si_3N_4, and Ti6Al4V. (PEEK and Ti6Al4V-ELI data are from References 42 and 43, respectively.).

negative charge (−70 mV), followed by N_2-SN (−65 mV), PEEK (extrapolated to −50 mV using non-linear regression analysis), Af-SN (−45 mV), and the Ti-alloy (−15 mV).

Wettability and water contact angle

Representative photos of deionized water contact angles for the various Si_3N_4, PEEK, and Ti-alloy samples are shown in Figure 5(a∼f). As expected, PEEK was the least hydrophilic material and had the poorest wettability, with a contact angle of 86 ± 4°. This was followed by the Ti-alloy, and Af-SN samples at 71 ± 5° and 66 ± 12°, respectively. However, it should be noted that prior work demonstrated that the apparent high contact angle for the Af-SN sample actually decreases to 30 ± 9° after 30 mins of exposure due to heterogeneous wetting (that is, air entrapment) of the micro-rough surface.[34,44] The three Si_3N_4 treatment conditions resulted in remarkable improvements in hydrophilicity, with contact angles of 28 ± 14°, 9 ± 2°, and 8 ± 1°, for the Gl-SN, N_2-SN, and Ox-SN samples, respectively.

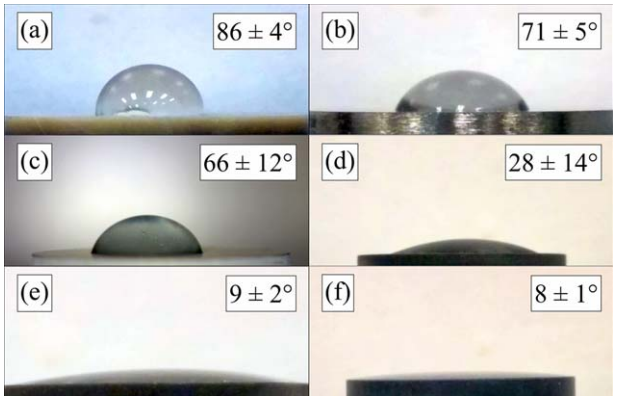

FIGURE 5. Water droplet wetting angle photographs and measurements: (a) PEEK, (b) Ti6Al4V-ELI, (c) Af-Si_3N_4, (d) Gl-Si_3N_4, (e) N_2-Si_3N_4, and (f) Ox-Si_3N_4. Measured values are mean ± one standard deviation.

TABLE II. Surface elemental composition via XPS for the as-fabricated and treated Si_3N_4 surfaces. The Si_3N_4 material's theoretical bulk composition is included for reference

	Surface elemental composition (Atomic %)				
Element	Theoretical bulk	Af-SN	N_2-SN	Gl-SN	Ox-SN
Si	39.7%	38.87%	36.41%	28.06%	34.53%
Y	1.1%	0.12%	2.30%	10.86%	1.37%
Al	1.6%	2.34%	5.66%	3.38%	3.06%
O	4.5%	19.39%	18.52%	33.10%	60.93%
N	52.9%	39.28%	37.11%	24.60%	0.11%

X-ray photoelectron spectroscopy

Results of the surface chemical analyses using XPS are provided in Table II for the various Si_3N_4 samples. The theoretical bulk composition is also listed. Of particular note is the significant amount of oxygen present on all of the treated samples (that is, from 19 at % to 61 at %). A protective oxide surface layer was a natural consequence of the material's exposure to ambient air (cf., Table II, Af-SN and N_2-SN); but this oxide coating was greatly enhanced using the glazing and oxidizing treatment conditions. Trends can also be noted for nitrogen, yttrium, and aluminum, with the Af-SN and N_2-SN samples containing the highest amounts of N, and the Gl-SN sample possessing the largest quantities of yttrium and aluminum. Specific moieties, including Si-NH_3^+, Y-OH_2^+, and Al-OH_2^+ intermixed with the predominant Si-O^- groups, form from the reaction of the surface with biological fluids at physiologic pH and engender the surface with a zwitterionic-like character. As will be discussed later, these specific surface chemistry changes may have an impact on the material's bacteriostatic capabilities. The elemental XPS results from the PEEK and Ti-alloy (not shown) were as expected. Their surface compositions consisted principally of C and O, and oxides of Ti, Al, and V, respectively.

Biofilm formation

Bacterial attachment and proliferation results at 24 h and 48 h for gram-positive *S. epidermidis* and gram-negative *E.*

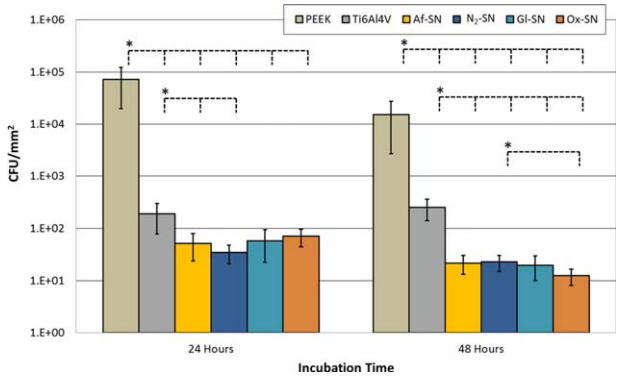

FIGURE 6. Bacteriostasis results on tested biomaterials using *S epi* after 24 and 48 h incubation. (Error bars are ± one standard deviation. Asterisks (*) in the figure indicate a statistically significant difference, $p < 0.05$. The position of each asterisk indicates the reference material used in the statistical analysis.).

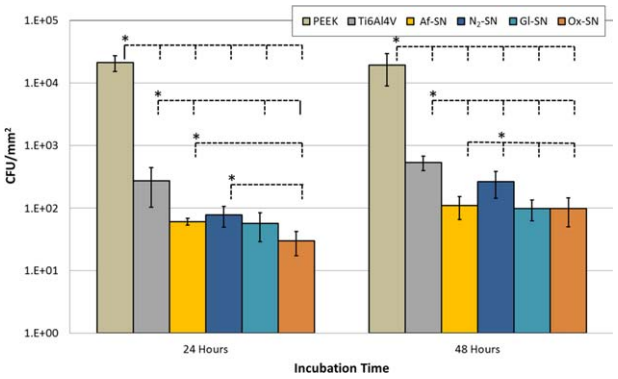

FIGURE 7. Bacteriostasis results on tested biomaterials using *E. coli* after 24 and 48 h incubation. (Error bars are ± one standard deviation. Asterisks (*) in the figure indicate a statistically significant difference, $p < 0.05$. The position of each asterisk indicates the reference material used in the statistical analysis.).

coli are given in Figures 6 and 7, respectively. Both microbial species showed similar biofilm forming trends. In general, the highest density of CFUs was always found on the PEEK biomaterial, followed by the Ti-alloy, and then the various Si_3N_4 substrates.

For *S. epidermidis* at 24 h, biofilm growth on PEEK was about three orders of magnitude greater than on the Ti-alloy or any Si_3N_4 material (all $p < 0.005$). Ti6Al4V also had more bacteria than the Si_3N_4 samples, but was only significant for as-fired and nitrogen annealed treatments (that is, p-values 0.048 and 0.035, respectively). There were no significant differences between any of the Si_3N_4 conditions at 24 h. Similar trends and statistical significance for *S. epidermidis* were also observed at 48 h. However, it was noted that the average *S. epidermidis* CFU/mm^2 values were lower at 48 h than at 24 h (cf., Figure 6). While this observation may seem contradictory, it was primarily the result of the chosen experimental protocol. The 24 h and 48 h data were derived from independent experiments and not the result of an extraction of samples from the same continuous experiment. Consequently, the observed CFU counts were subject to minor variations in the initial bacterium concentration and in the biogenic growth medium. In fact, comparing 24 h and 48 h results for individual materials presented no statistical differences.

For *E. coli*, biofilm formation on PEEK was significantly greater ($p < 0.05$) than all other materials at both 24 and 48 h. Bacterial growth on Ti6Al4V was also statistically greater ($p < 0.05$) than all Si_3N_4 conditions, with the possible exception of nitrogen annealed Si_3N_4 ($p = 0.06$). By 48 h, PEEK remained two orders of magnitude above the Ti-alloy, and 2.5–3 orders of magnitude greater than all of the Si_3N_4 conditions ($p < 0.05$); and Ti6Al4V was also significantly greater than all of the Si_3N_4 treatments at 48 h ($p < 0.05$).

DISCUSSION

In this study, a series of surface-modulated Si_3N_4 samples was prepared and extensively characterized prior to *in vitro* exposure to two common nosocomial bacterial strains in an attempt to gain an improved understanding of the surface parameters that may affect biofilm formation. Attachment of bacteria to biomaterial surfaces is complex, and correlations to single parameters are often difficult to assess.[13] Indeed, the literature is resplendent with *in vitro* studies that are inconsistent, inconclusive, and even contradictory.[11,21] Furthermore, while standard tests exist for assessing the bactericidal effectiveness of compounds,[45–47] none currently exist for generally determining a biomaterial's natural resistance to a range of biofilm forming microbes. Consequently, a multivariate approach is often necessary because microbial adhesion is not only related to the bacterial strain itself, but can also be affected by the biomaterial's surface topography, charging, wetting behavior, chemistry, and the *in vivo* environment (for example, serum proteins, nutrients, and fluid-flow conditions).

Surface topography

A biomaterial's surface topography is generally considered to be an important parameter in biofilm formation. Features such as crevices, asperities, voids, or porosity on the order of the size of the bacteria are believed to provide shelter against biological fluid flow (that is, shear) and phagocytes.[13,48] In contrast to the size of eukaryotic cells which have typical diameters of between 10 μm and 100 μm, bacteria are miniscule, with cell dimensions of about 0.2 μm in diameter × 2–8 μm length. These prokaryotic cells are more rigid than their mammalian counterparts, so it stands to reason that their initial adhesion to a biomaterial's surface may be different, and likely affected by topographical features. A generally-held axiom is that smoother, porosity free surfaces have fewer topographical defects where bacterial adhesins can take hold and cells can colonize.[21] This apparent truism has been validated by a number of researchers. For instance, Scheuerman et al. demonstrated enhanced adhesion of *P. aeruginosa* and *P. fluorescens* on micro-roughened silicon coupons.[49] Separate extensive reviews by Teughels et al. and Quirynen et al. showed that adherence of most strains of oral bacteria are strongly correlated to the surface roughness of implanted dental appliances.[50,51] In a more recent orthopaedic study, Yoda et al. tested five different metallic and ceramic biomaterials with a range of surface roughness values that varied between 2.1× and 4.0×. The rougher materials resulted in significantly greater adhesion and proliferation of *S. epidermidis*.[52] In contrast, the results of the present study, which included a similarly broad range of roughness values, appear to contradict the findings of these earlier researchers. Indeed, the Si_3N_4 samples had R_a values ranging from 509 to 785 nm, whereas the PEEK and Ti-alloy materials were conspicuously different at 819 and 377 nm, respectively. If high average surface roughness was the sole determinant of bacterial adhesion, then the Ti-alloy should have had the lowest amount of biofilm; the highest amount should have been observed on PEEK and all of the Si_3N_4 samples (cf., Table I, Figures (3 and 6), and 7). Clearly, this was not the case; the PEEK and Ti-alloy showed the largest amount of biofilm

formation for both bacterial species. However, average roughness may not be the appropriate measure. A close comparison of Figures 2 and 3 demonstrates that there are inherent differences in feature sizes between the Si_3N_4 materials and either the Ti-alloy or PEEK. The latter two materials have regular (that is, machined) features that are at least an order of magnitude larger than are the submicron- and nano-sized structures found on the Si_3N_4 surfaces. Studies have demonstrated that slight differences between nano-rough and nano-smooth surfaces may be important in limiting initial adhesion, with the former surface preventing attachment.[21] It has also been suggested that there may be an optimal feature size that either promotes or inhibits bacterial adhesion. Surfaces with roughness values in the plus-micrometer or in the low-nanometer ranges showed increased bacteria attachment in contrast to sub-micrometer roughness.[53] In a recent report, Xu et al. found that *S. epidermidis* biofilm formation was minimized by creating a regular array of submicron-sized pillars on hydrophobic polyurethane.[28] Then, in a subsequent article, they fashioned a larger micron-sized array of the same pillars, and plasma treated the polyurethane surface to improve its hydrophilicity. In this later case, *S. epidermidis* adhesion was found to be dependent upon the size of the textured pattern; submicron patterns reduced adhesion, whereas micron-sized arrays resulted in the opposite effect.[54] Other researchers have demonstrated similar results on different materials. Puckett et al. found that nano-rough titanium surfaces are more effective in repelling microbial adhesion than nano-smooth materials of the same composition.[55] In fact, these recent efforts have mimicked surfaces found in the natural world, such as the wings of the common cicada (insect) or the leaves of the lotus plant, both of which have intrinsic antibacterial properties due to nano-rough pillar-like patterns on their respective surfaces.[11,24,56,57] Due to multivariate effects, it is impossible to suggest that surface roughness is the sole determinant of the observed differences in microbial attachment between PEEK, Ti6Al4V, and the Si_3N_4 surfaces of the present study. However, it undoubtedly has a role, although its precise contributions cannot be quantitatively assessed.

Surface charge and wetting behavior

As indicated in Figure 1, bacterial adhesion to biomaterials consists of the initial attraction of the microbial species to the surface (Step 1) followed by adsorption and attachment (Step 2). In their planktonic state, their motility is affected by various physical and electrokinetic forces, including Brownian motion, van der Waals attraction, Columbic attraction or repulsion, and even gravity.[13,58] Several analytical models have been developed to explain their movement and attachment mechanisms, the most advanced of which is the Extended DLVO theory.[48,59,60] Within the biological medium, it accounts for electrokinetic interactions of individually dispersed bacterium and the prosthetic surface including surface roughness, hydrophilic, and hydrophobic effects. As a bacterium approaches the surface, it is either electrostatically attracted or repulsed based on the net effect of its surface charge and that of the biomaterial. While surface chemistry of individual bacterial species varies, all are heterogeneous combinations of positively-, neutrally-, or negatively-charged moieties. Their predominant surface groups include amines ($R\text{-}NH_3^+$), phosphates ($R\text{-}PO_4^{2-}$), hydroxyls ($R\text{-}O^-$), and carboxylates ($R\text{-}COO^-$).[61] Most bacterial genera have an overall negative surface charge which provides them with their electrophoretic mobility. Yet, given that many biomaterial surfaces are also negatively charged at homeostatic pH, a double-layer electrostatic repulsion is thought to prevent immediate attachment.[62] The extended-DLVO theory has been extensively used to model bacilli movement and attachment.[21] It is generally observed that highly hydrophilic biomaterial surfaces possessing large negative zeta-potentials are less prone to bacterial attachment and biofilm formation.[13] As an example, in their study of metal oxide and glass surfaces, Li et al. found that the measurement of only two parameters, wetting behavior and zeta-potential, were needed to predict differences in adhesion among eight different microbial strains.[29] Separately, Harkes, et al. studied the adhesion of three strains of *E. coli* on polymethacrylates of differing surface charges and hydrophobicities under laminar flow conditions.[63] They uniformly observed fewer bacteria on substrates with larger negative zeta-potentials, suggesting that the magnitude of the charge difference prevented the microbes from contacting the biomaterial's surface. They also found that substrates with large negative zeta-potentials also had improved wetting behavior. Such a result is not uncommon because charging and wettability are both directly related to the chemical moieties present at the surface. On the one hand, the biomaterial's crystal structure, lattice defects, broken surface bonds, and the ionization of attached functional groups determines its charge. On the other hand, it is dissociation or protonation of carboxyl, phosphate, and amino groups on cell membranes that govern the surface charge of most bacteria.[60] A number of studies have established that pathogen adhesion correlates with surface hydrophobicity, and in turn, poor wetting behavior is the primary etiology for biofilm formation.[64] While there are exceptions, microbial cell attachment is predominately impeded when the bacterial membrane and biomaterial surface both possess negative charges.[13] Furthermore, it is commonly observed that bacteria with hydrophobic properties prefer hydrophobic biomaterials, while hydrophilic bacilli prefer hydrophilic surfaces.[13,38] In any event, upon implantation of an abiotic biomaterial, a competition between bacteria, serum proteins, and eukaryotic cells ensues, known as a "race to the surface."[65] If the surface is hydrophilic and highly hydrated (that is, adsorbed water) or hydroxylated (that is, chemically bound water), then it may be energetically unfavorable for bacteria to gain a foothold. Conversely, no such adhesion barriers exist for hydrophobic surfaces. The results of the present study tend to support these general observations. In considering the combined effects of zeta-potential and wetting, the Si_3N_4 samples had both the charging and hydrophilicity characteristics to hinder bacterial attachment. For instance, the Ox-Si_3N_4 samples had the overall lowest

bacterial adhesion after 48 h incubation for both *S. epidermidis* and *E. coli*, the largest negative ζ-potential (≈−70 mV) at homeostatic pH, and the lowest measured wetting angle ($8 \pm 1°$). The other Si_3N_4 samples also had relatively large negative ζ-potentials (≈-50 mV) and advantageous hydrophilicity ($< 60°$). Conversely, the PEEK and Ti-alloy had ζ-potentials and wetting angles of ∼50 mV and $86 \pm 4°$, and −15 mV and $71 \pm 5°$, respectively. Although the ζ-potential for PEEK appears to be comparable to the Si_3N_4 samples, the mechanism for PEEK charging is completely different from that of the inorganic ceramic and metal samples. While inorganic materials become charged in aqueous environments due primarily to acid-base interactions between fixed (non-adsorbed) surface sites and the medium, PEEK's charge is solely due to adsorption of ions from solution. Consequently, unlike inorganic substances, its ζ-potential is determined primarily by its surface area and the relative concentrations of adsorbed species, with a rougher surface unduly increasing its apparent value.[66] Additionally, the biologic medium contains a much different and more concentrated ionic composition than the 1 mM KCl solution used in conducting the streaming potential experiments. While the inorganic materials are expected to exhibit lower magnitude zeta potentials in higher ionic strength media, their general behavior as a function of pH (relative to one another) is expected to remain comparatively constant. Since PEEK's charging behavior is dictated by the medium's ionic composition and ion adsorption, the reported data from a 1 mM KCl *in vitro* test is neither representative of the actual *in vivo* medium, nor is it comparable to the behavior of inorganic materials within the same medium. Consequently, even though the *in vitro* ζ-potential for PEEK is included in Figure 4 for reference, its *in vivo* value is expected to be neutral to <10 mV, similar to other untreated polymeric materials.[66,67] In summary, the results of this study for surface charging, hydrophilic behavior, and associated biofilm formation are consistent with previous research involving these and similar biomaterials.[29,32,33,68] They support the concept that highly hydrophilic surfaces with large negative ζ-potentials preclude microorganism attachment. It is therefore believed that these two surface properties strongly contributed to the bacteriostatic effectiveness of the Si_3N_4 materials in comparison to the PEEK and Ti-alloy. Nevertheless, their relative contributions have to be considered as part of a multivariate solution, because bacteria are more capable than simple colloidal particles in overcoming electrostatic and surface energy effects. Their living nature, motility, and functional extremities (capsule, fimbriae, and pili) which serve as adhesins, can defeat repulsive abiotic material barriers.[69,70]

Surface chemistry

Beyond electrostatic and hydrophilic effects, a biomaterial's functional surface chemistry can also be effective in preventing biofilm formation. For instance, polymer coatings containing primary through quaternary amines (for example, chitosan, peptides, *N*-halamines) have been shown to be contact biocides.[71] Although their exact mechanisms are still subject to debate, the rapid electrostatically-driven binding of bacteria to these polycationic compounds appears to impair the bacterium's outer cell membrane and increase its permeability, which leads to leakage of cytoplasmic constituents, the downregulation of cell metabolism, and eventual lysis.[72–74] The mechanism in *N*-halamines is slightly different but with the same end result; their antimicrobial action is due to the slow release of cationic oxidative halogen species (for example, Cl^+, Br^+) which, upon direct contact with bacteria, inactivates their cellular functions leading to eventual death.[71] Although the effectiveness of these types of materials increases with their functional group concentration, they are still only considered to be bacteriostatic, not bactericidal, because extended contact times are generally required to kill the adsorbed microbes.[72,73] Conversely, biomaterials coated or impregnated with elutable biocides (for example, silver, zinc, copper, iodine, nitric oxide, or synthetic antibiotics) are strongly bactericidal,[10] with similar lytic mechanisms involving disruption of cell membranes, leakage of constituents, and reduced metabolic activity. On the one hand, the use of silver compounds has been shown to be highly effective in preventing biofilm formation; but concerns remain about argyria and potential hepatoxicity, with long-term effects on mammalian cells remaining unknown.[2,10] On the other hand, nitric oxide releasing surfaces were equally bactericidal, and were actually shown to improve the biocompatibility of implanted medical devices.[75] Nevertheless, the lasting effectiveness of elution-based bactericidal surfaces is questioned. The gradual loss of their functional elements obviously diminishes their antimicrobial usefulness over time. However, the placement of specific chemical moieties at the surface of a biomaterial (either as a coating, or inherently as part of the monolithic implant) represents an important strategy in regulating the attachment of bacteria on substrates and their growth into biofilms.

In this regard, the Si_3N_4 samples utilized in the present study cannot be considered wholly bioinert. Indeed, unlike the PEEK and Ti6Al4V materials, the chemistry of Si_3N_4's surface is bioactive. Not only can its surface be broadly modulated (from one that is principally silicon dioxide (SiO_2) to one that has high concentrations of silicon-amines ($Si\text{-}NH_2$), and/or a silicon-yttrium-aluminum-oxynitride glass (SiYAlON)) but it also exhibits a certain degree of surface solubility.[76–80] As demonstrated in Figures 4 and 5 and as documented in Table II, chemical modulation of its surface results in significant alterations to its electrokinetic and wetting behavior, respectively. Note in particular that higher surface concentrations of oxygen led to a large negative surface charge and improved wettability consistent with the formation of a thicker silica-like layer (cf., Ox-SN in Table II and Figures 4 and 5). In a recent study, Katsikogianni and Missirlis found that hydroxyl-based (that is, OH-terminated) glass was highly effective in preventing adhesion of *S. epidermidis*; they attributed their findings to the mutually repulsive electrochemistry of the bacteria and the glass surface.[59] The present study appears to corroborate their results because the oxidized silicon nitride surface (that is,

Ox-SN) had among the lowest CFU counts at both 24 and 48 h for the two studied pathogens (cf., Figures 6 and 7).

Similarly, improved wetting, large negative charging, and reduced biofilm formation was also achieved through increased amounts of SiYAlON glass at the surface (cf., N_2-SN and Gl-SN in Table II, and Figures 4–7). Hydrophilicity and charging undoubtedly had a role in the reduction of these bacilli, but inclusion of specific positively charged surface functional groups (for example, Si-NH_3^+, Y-OH_2^+, and Al-OH_2^+) intermixed with the predominately negative Si-O^- charges provided the surface with zwitterionic-like characteristics. It is believed that this unique chemistry aided in inhibiting bacterial attachment as well. In fact, other researchers have demonstrated similar anti-infective behavior with zwitterionic surfaces. For instance, Izquierdo-Barba et al. examined the resistance of mesoporous silica surfaces to *Escherichia coli* adhesion after the surfaces had been functionalized with $-NH_3 \pm COO^-$ or $NH_3 \pm SiO^-$ moieties. Their *in vitro* results demonstrated that the presence of both positive and negative charges led to reduced *E. coli* attachment.[81] In a separate study, Kyomoto et al. grafted a polyzwitterionic coating composed of poly(2-methacryloyloxyethyl phosphoryl-choline) onto vitamin E-blended highly cross-linked polyethylene and tested this surface for adhesion by two virulent gram-positive *Staphylococcus aureus* strains. They found a 100-fold reduction in adhesion due to the mixed-charge character of the grafted polymer.[67] Finally, in a separate comprehensive review, Schlenoff remarked that these synthetic zwitterionic surfaces are in fact bioinspired; they seek to replicate the anti-fouling behavior observed for many marine organisms.[82] Consequently, the engineered modulation of Si_3N_4's surface is believed to have had a role in hindering attachment of *S. epidermidis* and *E. coli* in the present study.

In addition to surface charge and wetting considerations, it has also been recently demonstrated that surface dissolution of Si_3N_4 also impacts bacterial adhesion and biofilm formation.[83] In the presence of moisture, there is a diffusion-limited thermodynamic driving force to convert silicon nitride to silicic acid ($Si(OH)_4$) and ammonia (NH_3) as indicated in Equation (1) below:

$$\begin{aligned} &Si_3N_4 + 12H_2O \rightarrow 3Si(OH)_4 + 4NH_3 \\ &\Delta G\ 298^{\circ}K = -565\ kJ/mol \end{aligned} \quad (1)$$

The release of NH_3 from the Si_3N_4 surface not only increases the local pH to ≈8.5, which deleteriously affects bacteria adhesion,[69] but it also affects their metabolism in a manner similar to the elution of nitric oxide (NO) from xerogel polymers.[83] Charville et al. demonstrated this in a study which examined the effect of NO release from fibrinogen-mediated xerogel coated glass slides on the adhesion of *S. aureus*, *S. epidermidis*, and *E. coli*.[84] At a NO flux of 30 pmol cm^{-2} s^{-1}, they found bacterial surface coverage reductions of 96%, 48% and 88%, respectively. The inhibitory mechanism was reportedly due to formation of peroxynitrite ($ONOO^-$), a highly reactive species, which penetrated the cells' lipid membranes resulting in leakage and causing irreparable damage to their metabolic respiration reactions and DNA.[85] Similarly, in a recent Raman spectroscopy study, Pezzotti, et al. monitored *in situ* the metabolic activity of *Porphyromonas gingivalis* inoculated onto various Si_3N_4 surfaces over a period of six days. Their results and the mechanism were consistent with the early study by Charville et al. for NO emitting xerogels. Pezzotti et al. concluded that the lytic activity was principally due to the formation of peroxynitrite. Its presence resulted in degradation of the cell membrane, alteration of internal protein structures, and interference with DNA and RNA metabolism.[83]

To summarize this section, it is believed that the surface chemistry of Si_3N_4 had a profound impact on the adhesion of the two nosocomial bacteria of this study. In keeping with the multivariate concept, modulation of the surface was shown to effect charging and wettability, both of which correlated with reduced pathogen adherence. In addition, it is further hypothesized that surface dissolution of Si_3N_4 generated ammonia and the concomitant formation of peroxynitrite. These reaction products resulted in a local increase in pH which inhibited bacterial adhesion and disrupted their cellular metabolic activity, respectively.

Proteins

At the onset, it was elected to include human plasma in this *in vitro* study because protein adsorption onto biomaterial surfaces can mediate the approach and adhesion of both prokaryotic and eukaryotic cells by preconditioning the surface. Although these experiments did not specifically examine the effect of proteins on bacterial attachment, the following discussion is provided as a reasonable interpretation of their potential effect on the results. Future studies will seek to quantify the impact of proteins on biofilm formation.

Human plasma may contain upwards of 40,000 unique proteins of which only about 1,000 have been cataloged.[41,86] Six abundant molecules account for 85% of its mass with an additional fourteen proteins comprising another 13%.[87] Those of pathological importance include albumin (55 to 70 wt %), fibrinogen (≈7 wt %), fibrin, fibronectin, laminin, and collagen.[86,88] Following hydration in a biological fluid, proteins are the first molecules to attach to an abiotic surface. This typically occurs within microseconds of implantation.[41] In accordance with the *Vroman Effect*, the first proteins are typically those that are plentiful and small (for example, albumin, immunoglobulins, and fibrin). Then, over time, these smaller proteins are replaced by larger molecules that have a higher affinity to the particular surface.[68] Although protein attraction and adhesion are largely concentration dependent, all are also subject to the same electrokinetic forces that affect bacteria, including ionic or electrostatic and hydrophobic-hydrophilic interactions. The Extended DLVO theory is equally applicable to both proteins and bacteria. Extensive studies have shown that hydrophilic, highly hydrated (for example, those with hydroxyl functional groups), and negatively charged surfaces are not only resistant to bacterial attachment, but also resistant to protein adsorption.[41] Although proteins have amphiphilic functional

groups capable of adsorbing onto either hydrophilic or hydrophobic surfaces, the energetics of surface dehydration may hinder actual adsorption from occurring on hydrogen bonded or hydroxylated materials. Therefore, water plays a key role in protein attachment. A number of wetting behavior studies have shown that there is an apparent pivot point in adsorption with a paucity of proteins found on surfaces having water contact angles of less than about 65°.[41] With regards to specific proteins, albumin (that is, the most abundant plasma molecule) reportedly improves the hydrophilicity of material surfaces, and also shows inhibitory tendencies toward bacterial attachment on most polymer, ceramic, and metal surfaces.[13,69] Conversely, fibrinogen or fibronectin are thought to facilitate adhesion of bacteria through specific ligand-receptor interactions,[64,69] although their ability to mediate bacterial attachment remains controversial, particularly for bacteria of the *staphylococci* genus.[14] In the previously cited study on the use of elutable nitric oxide, fibrinogen's ligand-receptor function was downregulated by NO, which led to its inability to facilitate binding of *S. aureus* and *S. epidermidis*.[84] Given these specific research findings, it is likely that there was minimal adsorption of plasma proteins onto the Si_3N_4 samples of the present study. This is thought to be primarily due to the large negative charge present at the Si_3N_4 surfaces along with their enhanced hydrophilicity. The localized increase in pH and formation of peroxynitrite via elution of silicic acid and ammonia may also have affected protein adsorption. In addition, albumin, because of its high plasma concentration, would likely have been the dominant adsorbate, leading to a further improvement in hydrophilicity of the Si_3N_4 surfaces. Therefore, it is altogether plausible that these combined effects would have further inhibited the adhesion of the two pathogens utilized in the present study. Future work will seek to better understand and quantify the roles of specific proteins on bacterial adhesion and biofilm formation for the various Si_3N_4 materials.

CONCLUSIONS

The present study investigated phenomenological differences for adhesion and biofilm formation of two nosocomial bacteria – *S. epidermidis* and *E. coli* – on three biomaterials routinely employed as intervertebral spacers in spinal fusion surgery – Si_3N_4, Ti6Al4V, and PEEK. Several surface modulated variants of Si_3N_4 were concurrently tested. The results demonstrated substantial differences in bacterial attachment and proliferation for both gram-positive *S epidermidis* and gram-negative *E coli*. Similar statistically significant trends were observed using both bacilli for incubation periods of 24 and 48 h. Biofilm formation was found to be the greatest on PEEK, followed by the Ti-alloy, and then the various Si_3N_4 treated surfaces. In particular, the amount of biofilm on the PEEK biomaterial remained approximately two orders of magnitude greater than Ti6Al4V, and 2.5 to 3 orders of magnitude above all of the Si_3N_4 variants at 48 h. Although detailed mechanistic studies were not a part of the present experiments (they are planned for the future), it is believed that multivariate effects resulted in the improved bacteriostasis behavior for the Si_3N_4 biomaterials. These effects included: (1) A submicron- nano-scale surface topography present on all of the Si_3N_4 samples in contrast to the micron-rough surfaces on the PEEK and Ti-alloy biomaterials; (2) Significantly larger negative surface charging for the Si_3N_4 samples in comparison to either PEEK or Ti6Al4V; (3) Improved wetting behavior for all of the Si_3N_4 materials when compared to PEEK and the Ti-alloy; and (4) Bioactive surfaces for the various Si_3N_4 samples, some of which exhibited zwitterionic-like character, eluted minute amounts of silicic acid and ammonia. With respect to the release of ammonia, a parallel dental bacteria study demonstrated that its elution from Si_3N_4 generated peroxynitrite, which in turn penetrated the pathogen and downregulated its cellular metabolism. In contrast, the PEEK and Ti6Al4V biomaterials were found to be essentially bioinert. Future studies will seek to: (1) Clarify the roles of these various mechanisms in suppressing bacterial adhesion and biofilm production; (2) Specifically examine the effects of protein adsorption on bacterial attachment; and (3) Test the bacteriostatic effectiveness of the various Si_3N_4 modulated surfaces over longer time intervals.

In summary, given the international threat associated with the impending ineffectiveness and critical shortages of new antibiotic therapies, identifying biomaterials that inherently or naturally resist biofilm formation and bacterial expression is an important strategy in addressing implant-related infections. Biomaterials, such as Si_3N_4, which possess multivariate bacteriostatic properties may provide clinicians and patients alike with a new effective remedy against an ever-increasing number of virulent microbial strains.

DISCLOSURES

Ryan M. Bock, Erin N. Jones, Darin A. Ray, B. Sonny Bal, and Bryan J. McEntire are principals or employees of Amedica Corporation, a silicon nitride orthopaedic device manufacturer. Giuseppe Pezzotti is a member of the Scientific Advisory Board of Amedica Corporation.

ACKNOWLEDGMENT

The authors gratefully acknowledge Dr. Brian van Devener of the University of Utah for performing XPS measurements and aiding in data analyses. Dr. Vinod Radhakrishnan of Anton-Paar USA is appreciated for performing streaming potential measurements. This work made use of University of Utah shared facilities of the Micron Microscopy Suite sponsored by the College of Engineering, Health Sciences Center, Office of the Vice President for Research, and the Utah Science Technology and Research (USTAR) initiative of the State of Utah.

REFERENCES

1. Matar WY, Jafari SM, Restrepo C, Austin M, Purtill JJ, Parvizi J. Preventing Infection in Total Joint Arthroplasty. J Bone Jt Surg 2010;92:36–46.
2. Gbejuade HO, Lovering AM, Webb JC. The role of microbial biofilms in prosthetic joint infections. Acta Orthop 2015;86:147–158.

3. Dowsey MM, Peel TN, Choong PFM. Infection in primary hip and knee arthroplasty. In: Fokter S. editor. Recent Adv Arthroplast. Published Online: Intechopen.com; 2012:413–438. DOI:10.5772.
4. Kurtz SM, Lau E, Schmier J, Ong KL, Zhao K, Parvizi J. Infection burden for hip and knee arthroplasty in the United States. J Arthroplasty 2008;23:984–991.
5. Kurtz SM, Lau E, Ong KL, Carreon L, Watson H, Albert T, Glassman S. Infection risk for primary and revision instrumented lumbar spine fusion in the medicare population. J Neurosurg Spine 2012;17:342–347.
6. Jaekel DJ, Ong KL, Lau EC, Watson HN, Kurtz SM. Epidemiology of total hip and knee arthroplasty infection. In: Bryan D. Springer and Javad Paravizi editor. Periprosthetic Joint Infection of the Hip and Knee. New York: Springer; 2014. DOI:10.1007/978-1-4614-7928-4_1.
7. Gutowski CJ, Chen AF, Parvizi J. The incidence and socioeconomic impact of periprosthetic joint infection: United States perspective. In: Kendoff D, Morgan-Jones R, Haddad SF, editors. Periprosthetic Joint Infections Changing Paradigms. Cham: Springer International Publishing; 2016.
8. Carlet J, Jarlier V, Harbarth S, Voss A, Goossens H, Pittet D. Ready for a world without antibiotics? The Pensières antibiotic resistance call to action. Antimicrob Resist Infect Control 2012;1:11.
9. Gandra S, Barter DM, Laxminarayan R. Economic burden of antibiotic resistance: How much do we really know? Clin Microbiol Infect 2014;20:973–979.
10. Vasilev K, Cook J, Griesser HJ. Antibacterial surfaces for biomedical devices. Expert Rev Med Devices 2009;6:553–567.
11. Campoccia D, Montanaro L, Arciola CR. A review of the biomaterials technologies for infection-resistant surfaces. Biomaterials 2013;34:8533–8554.
12. Bordi C, de Bentzmann S. Hacking into bacterial biofilms: A new therapeutic challenge. Ann Intensive Care 2011;1:1–8.
13. Katsikogianni M, Missirlis YF. Concise review of mechanisms of bacterial adhesion to biomaterials and of techniques used in estimating bacteria-material interactions. Eur Cells Mater 2004;8:37–57.
14. Moraes MN, Silveira WCD, Teixeira LEM, Araújo ID. Mechanisms of bacterial adhesion to biomaterials. Rev Médica Minas Gerais 2013;23:99–104.
15. Davies D. Understanding biofilm resistance to antibacterial agents. Nat Rev Drug Discov 2003;2:114–122.
16. Stewart PS, William Costerton J. Antibiotic resistance of bacteria in biofilms. Lancet 2001;358:135–138.
17. Stoodley P, Ehrlich GD, Sedghizadeh PP, Hall-Stoodley L, Baratz ME, Altman DT, Sotereanos NG, Costerton JW, DeMeo P. Orthopaedic biofilm infections. Curr Orthop Pract 2011;22:558–563.
18. Cobo J, Del Pozo JL. Prosthetic joint infection: Diagnosis and management. Expert Rev anti Infect Ther 2011;9:787–802.
19. Bazaka K, Jacob MV, Crawford RJ, Ivanova EP. Efficient surface modification of biomaterial to prevent biofilm formation and the attachment of microorganisms. Appl Microbiol Biotechnol 2012;95:299–311.
20. Hasan J, Crawford RJ, Ivanova EP. Antibacterial surfaces: The quest for a new generation of biomaterials. Trends Biotechnol 2013;31:295.
21. Desrousseaux C, Sautou V, Descamps S, Traoré O. Modification of the surfaces of medical devices to prevent microbial adhesion and biofilm formation. J Hosp Infect 2013;85:87–93.
22. Gomes J, Grunau A, Lawrence AK, Eberl L, Gademann K. Bioinspired surfaces against bacterial infections. Chim Int J Chem 2013; 67:275–278.
23. Bryers JD, Ratner BD. Bioinspired implant materials befuddle bacteria. ASM News 2004;70:232–237.
24. Ivanova EP, Hasan J, Webb HK, Truong VK, Watson GS, Watson JA, Baulin VA, Pogodin S, Wang JY, Tobin MJ, L??bbe C, Crawford RJ. Natural bactericidal surfaces: Mechanical rupture of pseudomonas aeruginosa cells by cicada wings. Small 2012;8:2489–2494.
25. Carvalho I, Henriques M, Carvalho S. New strategies to fight bacterial adhesion. In: Mendez-Vilas A, editor. Microbial Pathogens and Strategies Combating Them: Science, Technology and Education. Formatex; 2013.
26. An YH, Friedman RJ. Concise review of mechanisms of bacterial adhesion to biomaterial surfaces. J Biomed Mater Res 1998;43: 338–348.
27. Anselme K, Davidson P, Popa AM, Giazzon M, Liley M, Ploux L. The interaction of cells and bacteria with surfaces structured at the nanometre scale. Acta Biomater 2010;6:3824–3846.
28. Xu L-C, Siedlecki CA. Submicron-textured biomaterial surface reduces staphylococcal bacterial adhesion and biofilm formation. Acta Biomater 2012;8:72–81.
29. Li B, Logan BE. Bacterial adhesion to glass and metal-oxide surfaces. Colloids Surfaces B, Biointerfaces 2004;36:81–90.
30. Arciola CR, Campoccia D, Speziale P, Montanaro L, Costerton JW. Biofilm formation in staphylococcus implant infections. a review of molecular mechanisms and implications for biofilm-resistant materials. Biomaterials 2012;33:5967–5982.
31. Cremet L, Corvec S, Bemer P, Bret L, Lebrun C, Lesimple B, Miegeville AF, Reynaud A, Lepelletier D, Caroff N. Orthopaedic-implant infections by Escherichia coli: Molecular and phenotypic analysis of the causative strains. J Infect 2012;64:169–175.
32. Webster TJ, Patel AA, Rahaman MN, Bal BS. Anti-infective and osteointegration properties of silicon nitride, poly (ether ether ketone), and titanium implants. Acta Biomater 2012;8:4447–4454.
33. Gorth DJ, Puckett S, Ercan B, Webster TJ, Rahaman M, Bal BS. Decreased bacteria activity on Si_3N_4 Surfaces compared with PEEK or titanium. Int J Nanomedicine 2012;7:4829–4840.
34. Bock RM, McEntire BJ, Bal BS, Rahaman MN, Boffelli M, Pezzotti G. Surface modulation of silicon nitride ceramics for orthopaedic applications. Acta Biomater 2015;26:318–330.
35. Bal BS, Rahaman MN. Orthopedic applications of silicon nitride ceramics. Acta Biomater 2012;8:2889–2898.
36. Neoh KG, Hu X, Zheng D, Kang ET. Balancing osteoblast functions and bacterial adhesion on functionalized titanium surfaces. Biomaterials 2012;33:2813–2822.
37. Rao PJ, Pelletier MH, Walsh WR, Mobbs RJ. Spine interbody implants: Material selection and modification, functionalization and bioactivation of surfaces to improve osseointegration. Orthop Surg 2014;6:81–89.
38. Moucha CS. Antibacterial surface treatment for orthopaedic implants. Int J Mol Sci 2014;15:13849–13880.
39. Delgado AV, González-Caballero F, Hunter RJ, Koopal LK, Lyklema J. Measurement and interpretation of electrokinetic phenomena. J Colloid Interface Sci 2007;309:194–224.
40. Arciola CR. Titanium oxide antibacterial surfaces in biomedical devices. Int J Artif Organs 2011;34:929–946.
41. Vogler EA. Protein adsorption in three dimensions. Biomaterials 2012;33:1201–1237.
42. Waser-Althaus J, Salamon A, Waser M, Padeste C, Kreutzer M, Pieles U, Muller B, Peters K. Differentiation of human mesenchymal stem cells on plasma-treated polyetheretherketone. J Mater Sci Mater Med 2014;25:515–525.
43. Roessler S, Zimmermann R, Scharnweber D, Werner C, Worch H. Characterization of oxide layers on Ti6Al4V and titanium by streaming potential and streaming current measurements. Colloids Surfaces B Biointerfaces 2002;26:387–395.
44. Marmur A. Wetting on hydrophobic rough surfaces: To be heterogeneous or not to be? Langmuir 2003;19:8343–8348.
45. ISO 22196:2011, Measurement of antibacterial activity on plastics and other non-porous surfaces, International Organization for Standardization, Geneva, Switzerland, 2016.
46. ASTM E2149 - 13a, Standard test method for determining the antimicrobial activity of antimicrobial agents under dynamic contact conditions. ASTM Innternational. West Conshohocken, PA USA. 2016.
47. ASTM E2180 - 07(2012), Standard test method for determining the activity of incorporated antimicrobial agent(s) in polymeric or hydrophobic materials. ASTM International. West Conshohocken, PA USA. 2016.
48. Missirlis YF, Katsikogianni M. Theoretical and experimental approaches of bacteria-biomaterial interactions. Materwiss Werksttech 2007;38:983–994.
49. Scheuerman TR, Camper AK, Hamilton MA. Effects of substratum topography on bacterial adhesion. J Colloid Interface Sci 1998; 208:23–33.
50. Teughels W, Assche N, Sliepen I, Quirynen M. Effect of material characteristics and/or surface topography on biofilm development. Clin Oral Implants Res 2006;17(Suppl 2):68–81.

51. Quirynen M, Bollen CML. The influence of surface roughness and surface-free energy on supra- and subgingival plaque formation in man. J Clin Periodontol 2005;22:1–14.
52. Yoda I, Koseki H, Tomita M, Shida T, Horiuchi H, Sakoda H, Osaki M. Effect of surface roughness of biomaterials on staphylococcus epidermidis adhesion. BMC Microbiol 2014;14:234.
53. Truong VK, Rundell S, Lapovok R, Estrin Y, Wang JY, Berndt CC, Barnes DG, Fluke CJ, Crawford RJ, Ivanova EP. Effect of ultrafine-grained titanium surfaces on adhesion of bacteria. Appl Microbiol Biotechnol 2009;83:925–937.
54. Xu L-C, Siedlecki CA. *Staphylococcus epidermidis* Adhesion on Hydrophobic and Hydrophilic Textured Biomaterial Surfaces. Biomed Mater 2014;9:35003.
55. Puckett SD, Taylor E, Raimondo T, Webster TJ. The relationship between the nanostructure of titanium surfaces and bacterial attachment. Biomaterials 2010;31:706–713.
56. Kelleher SM, Habimana O, Lawler J,O, Reilly B, Daniels S, Casey E, Cowley A. Cicada wing surface topography: an investigation into the bactericidal properties of nanostructural features. ACS Appl Mater Interfaces 2015;acsami.5b08309.
57. Watson GS, Green DW, Sun M, Liang A, Xin L, Cribb BW, Watson JA. The insect (cicada) wing membrane micro/nano structure – nature's templates for control of optics, wetting, adhesion, contamination, bacteria, and eukaryotic cells. J Nanosci with Adv Technol 2015;1:6–16.
58. Renner LD, Weibel DB. Physicochemical regulation of biofilm formation. MRS Bull 2011;36:347–355.
59. Katsikogianni MG, Missirlis YF. Interactions of bacteria with specific biomaterial surface chemistries under flow conditions. Acta Biomater 2010;6:1107–1118.
60. Poortinga AT, Bos R, Norde W, Busscher HJ. Electric double layer interactions in bacterial adhesion to surfaces. Surf Sci Rep 2002; 47:1–32.
61. Hong Y, Brown DG. Electrostatic behavior of the charge-regulated bacterial cell surface. Langmuir 2008;24:5003–5009.
62. Zhang X, Wang L, Levänen E. Superhydrophobic surfaces for reduction of bacterial adhesion. RCS Adv 2013;3:12003.
63. Harkes G, Feijen J, Dankert J. Adhesion of Escherichia coli on to a series of poly(methacrylates) differing in charge and hydrophobicity. Biomaterials 1991;12:853–860.
64. Gittens RA, Scheideler L, Rupp F, Hyzy SL, Geis-Gerstorfer J, Schwartz Z, Boyan BD. A review on the wettability of dental implant surfaces II: Biological and clinical aspects. Acta Biomater 2014;10:2907–2918.
65. Gristina AG. Biomaterial-centered infection: Microbial adhesion versus tissue integration. Science 1987;237:1588–1595.
66. Weidenhammer P, Jacobasch H-J. Investigation of adhesion properties of polymer materials by atomic force microscopy and zeta potential measurements. J Colloid Interface Sci 1996;180:232–236.
67. Kyomoto M, Shobuike T, Moro T, Yamane S, Takatori Y, Tanaka S, Miyamoto H, Ishihara K. Prevention of bacterial adhesion and biofilm formation on a vitamin E-blended, cross-linked polyethylene surface with a poly(2-methacryloyloxyethyl phosphorylcholine) layer. Acta Biomater 2015;24:24–34.
68. Rochford ETJ, Poulsson AHC, Salavarrieta Varela J, Lezuo P, Richards RG, Moriarty TF. Bacterial adhesion to orthopaedic implant materials and a novel oxygen plasma modified PEEK surface. Colloids Surfaces B Biointerfaces 2014;113:213–222.
69. Ribeiro M, Monteiro FJ, Ferraz MP. Infection of orthopedic implants with emphasis on bacterial adhesion process and techniques used in studying bacterial-material interactions. Biomatter 2012;2:176–194.
70. Donlan RM. Biofilms: Microbial life on surfaces. Emerg Infect Dis 2002;8:881–890.
71. Timofeeva L, Kleshcheva N. Antimicrobial polymers: Mechanism of action, factors of activity, and applications. Appl Microbiol Biotechnol 2011;89:475–492.
72. Rabea EI, Badawy MET, Stevens CV, Smagghe G, Steurbaut W. Chitosan as antimicrobial agent: Applications and mode of action. Biomacromolecules 2003;4:1457–1465.
73. Raafat D, von Bargen K, Haas A, Sahl H-G. Insights into the mode of action of chitosan as an antibacterial compound. Appl Environ Microbiol 2008;74:3764–3773.
74. Kong M, Chen XG, Xing K, Park HJ. Antimicrobial properties of chitosan and mode of action: A state of the art review. Int J Food Microbiol 2010;144:51–63.
75. Frost MC, Reynolds MM, Meyerhoff ME. Polymers incorporating nitric oxide releasing/generating substances for improved biocompatibility of blood-contacting medical devices. Biomaterials 2005;26:1685–1693.
76. Laarz E, Zhmud BVB, Bergström L, Bergstrom L. Dissolution and deagglomeration of silicon nitride in aqueous medium. J Am Ceram Soc 2000;83:2394–2400.
77. Zhmud BV, Bergström L. Dissolution kinetics of silicon nitride in aqueous suspension. J Colloid Interface Sci 1999;218:582–584.
78. Mazzocchi M, Gardini D, Traverso PL, Faga MG, Bellosi A. On the possibility of silicon nitride as a ceramic for structural orthopaedic implants. Part II: Chemical stability and wear resistance in body environment. J Mater Sci Mater Med 2008;19:2889–2901.
79. Dante RC, Kajdas CKA. Review and a fundamental theory of silicon nitride tribochemistry. Wear 2012;288:27–38.
80. Özmen Y. Si3N4 as a biomaterial and its tribo-characterization under water lubrication. Lubr Sci 2016;28:243–254.
81. Izquierdo-Barba I, Sánchez-Salcedo S, Colilla M, Feito MJ, Ramírez-Santillán C, Portolés MT, Vallet-Regí M. Inhibition of bacterial adhesion on biocompatible Zwitterionic SBA-15 mesoporous materials. Acta Biomater. Acta Materialia Inc 2011;7:2977–2985.
82. Schlenoff JB. Zwitteration: Coating surfaces with Zwitterionic functionality to reduce nonspecific adsorption. Langmuir 2014;30: 9625–9636.
83. Pezzotti G, Bock RM, McEntire BJ, Jones E, Boffelli M, Zhu W, Baggio G, Boschetto F, Puppulin L, Adachi T, Yamamoto T, Kanamura N, Marunaka Y, Bal BS. Silicon nitride bioceramics induce chemically driven lysis in porphyromonas gingivalis. Langmuir 2016;32:3024–3035.
84. Charville GW, Hetrick EM, Geer CB, Schoenfisch MH. Reduced bacterial adhesion to fibrinogen-coated substrates via nitric oxide release. Biomaterials 2008;29:4039–4044.
85. Watmough NJ, Butland G, Cheesman MR, Moir JWB, Richardson DJ, Spiro S. Nitric oxide in bacteria: Synthesis and consumption. Biochim Biophys Acta - Bioenerg 1999;1411:456–474.
86. Blood Basics [Internet]. Sigma Aldrich. 2016 [cited 2016 May 23]. Available from: http://www.sigmaaldrich.com/life-science/metabolomics/enzyme-explorer/learning-center/plasma-blood-protein/blood-basics.html
87. Lull ME, Freeman WM, Myers JL, Midgley F, Kimatian SJ, Undar A, Vrana KE. Plasma proteomics: A noninvasive window on pathology and pediatric cardiac surgery. ASAIO J 2006;52:562–566.
88. Anderson NL. The human plasma proteome: History, character, and diagnostic prospects. Mol Cell Proteomics 2002;1:845–867.